

Ab-Initio calculation of the interionic potential and phonons in aluminum: Breakdown of a convenient approach

G.J. Vázquez and L.F. Magaña

*Instituto de Física, Universidad Nacional Autónoma de México,
Apdo. Postal 20-364, 01000 México, D.F.*

(recibido el 17 de abril de 1986; aceptado el 16 de octubre de 1986)

Abstract. We have calculated from first principles the interionic potential of aluminum. The method we used is based on the density functional formalism and is an extension of the usual perturbative approach. The procedure uses nonlinear self-consistent calculations of the displaced electron charge density distribution around an external charge immersed in an electron gas. This method had been applied previously only to metallic hydrogen and lithium. From the calculated potential we obtained the phonon dispersion curves using the self-consistent harmonic approximation. The predictions of the phonons are far from experimental results showing that the method has to be refined in order to be applied to metals heavier than metallic hydrogen and lithium.

Resumen. Hemos calculado, de primeros principios, el potencial interiónico de aluminio. El método utilizado para calcularlo se basa en el formalismo de funcionales de la densidad y es una extensión del enfoque usual de teoría de perturbaciones. El procedimiento requiere de cálculos autoconsistentes y no-lineales de la densidad electrónica alrededor de una carga externa en un gas de electrones. Este método solamente había sido utilizado anteriormente en hidrógeno metálico y en litio. A partir de los potenciales calculados obtuvimos las curvas de dispersión de fonones por medio de la aproximación armónica autoconsistente. Las curvas de dispersión que resultan del cálculo quedan lejos de los resultados experimentales, mostrando así que el método tiene que refinarse para poder ser aplicado a metales más pesados que hidrógeno o litio.

PACS: 63.20-e

1. Introduction

A very important ingredient for the investigation of the properties of solids is the knowledge of the interionic potential. For the particular case of metals, several methods have been proposed [1–10] to find the interionic potentials. Some of them are based on the use of empirical potentials (Morse or Lennard–Jones type). These potentials show no Friedel oscillations and decay very rapidly.

Another often used approach for finding the interionic potential is by pseudopotentials and perturbation theory. In this approach we have empirical pseudopotentials and first principles pseudopotentials. At present it is known that a pseudopotential determined in an empirical way cannot always be considered as weak [11], so that its use in getting the interionic potential is not justified. The first principles pseudopotentials show Friedel oscillations and may be local, non-local or energy dependent.

In what is the usual approach to the calculation of the properties of simple metals, the starting point is a free electron gas into which bare pseudopotentials are introduced; these are treated self-consistently by perturbation theory. The resulting interionic potential can then be interpreted as the electrostatic interaction of one bare pseudopotential with a second screened one, with additional corrections for exchange and correlation. The screening cloud turns out to be the density distribution surrounding the ion when immersed in an otherwise uniform electron gas, but with wavefunctions calculated to first order in this perturbation.

The calculation of the interionic potential can be made from first principles using pseudopotentials [7, 8, 9]. This has been done using the density functional formalism [12, 13], to calculate the induced charge density around an ion in an electron gas. Then, a pseudopotential is chosen to reproduce the induced charge density in linear response, except in a region close to the ion, where the density has to be modelled. This modelling is not unique. In this way non-linear effects are partly included in the pseudopotential.

In this work we followed a method based on the density functional formalism for calculating the density around an ion in an electron gas. The interionic potential is given in terms of the density and the direct interaction between two ions. We don't use pseudopotentials. This method has been applied with success to metallic hydrogen [14] and with relative success to lithium [15]. From the resulting potential we obtained the phonon dispersion curves using the self consistent harmonic approximation [16].

The second part of this work is to describe briefly how to obtain the interionic potential. The set of equations to be solved in the self consistent harmonic approximation to calculate the phonon dispersion curves is presented in section 3. Finally, in section 4 we give the results and discussion.

2. The Interionic Potential

We explain the method briefly, for more details the reader may see Refs. 1, 14 and 15.

We start with an interacting and electrically neutral electron gas, represented by a Hamiltonian H and an average electronic density n_0 . We now add two static charges of magnitude Z to this system and, to preserve charge neutrality, $2Z$ electrons are also added. One of the static charges is located at the origin and the other at \mathbf{R} . The new total hamiltonian for the electron gas is H_T . Following a well known procedure (similar to that used in the proof of Hellmann-Feynman theorem [17]) the total energy change including the direct interaction Z^2/R between the two static charges and the differences between the ground state energies of the electrons described by H_T and H , respectively, can be written as

$$\Delta E_T = \frac{Z^2}{R} - Z \int_0^1 d\lambda \int d^3r \rho_\lambda(\mathbf{r}) \left[\frac{Z}{|\mathbf{r}|} + \frac{Z}{|\mathbf{r} - \mathbf{R}|} \right], \quad (1)$$

where we are using atomic units (double Rydbergs), $e = \hbar = m = 1$, where e and m are the electron charge and mass, \hbar is Plank's constant

divided by 2π , and

$$\rho_\lambda(\mathbf{r}) = \langle \Psi(\lambda) | \Psi^+(\mathbf{r}) \psi(\mathbf{r}) | \Psi(\lambda) \rangle, \quad (2)$$

where $|\Psi(\lambda)\rangle$ is the state vector for the ground state of the Hamiltonian $H(\lambda) = H + \lambda H'$, *i.e.*,

$$H(\lambda) |\Psi(\lambda)\rangle = E_{e1}(\lambda) |\Psi(\lambda)\rangle, \quad (3)$$

with $0 \leq \lambda \leq 1$.

In order to obtain ΔE_T given by Eq. (1) we need to calculate the electron density, $\rho_\lambda(\mathbf{r})$, for each value of λ between 0 and 1. Because of the difficulty of performing the two centres calculation for each \mathbf{R} , and guided by the usual method we assume that $\rho_\lambda(\mathbf{r})$ can be reasonably approximated by

$$\rho_\lambda(\mathbf{r}) \cong \Delta n_\lambda(\mathbf{r}) + \Delta n_\lambda(\mathbf{r} - \mathbf{R}) + n_0, \quad (4)$$

where $\Delta n_\lambda(\mathbf{r})$ is the displaced electron density around the charge sitting at the origin and $\Delta n_\lambda(\mathbf{r} - \mathbf{R})$ is the displaced electron density around the charge at \mathbf{R} , n_0 is the unperturbed electron density.

Substituting Eq. (4) in Eq. (1), neglecting additive constants and terms which are \mathbf{R} independent and using spherical symmetry, we get for the interionic potential, $V(R)$:

$$V(R) = \frac{Z^2}{R} - 2Z \int_0^1 d\lambda [F_1(\lambda, R) + F_2(\lambda, R)], \quad (5)$$

where

$$F_1(\lambda, R) \equiv \int_0^R \frac{4\pi r^2 \Delta n_\lambda(r)}{R} dr \quad (6)$$

and

$$F_2(\lambda, R) \equiv \int_R^\infty 4\pi r \Delta n_\lambda(r) dr. \quad (7)$$

The expression for $V(R)$ given by Eq. (5) is the one we use for the interionic potential.

To calculate $\Delta n_\lambda(r)$, which is the displaced electron density in an electron gas perturbed by a single charge λZ at the origin we use the formalism of Hohenberg-Kohn and Sham [12, 13]. We can calculate $\Delta n_\lambda(r)$ in terms of the self consistent solutions $\psi_i(r)$ of a Schrödinger equation,

$$-\left[-\frac{1}{2}\nabla^2 + V_{\text{eff}}(\mathbf{r})\right] \psi_i(\mathbf{r}) = E_i \psi_i(\mathbf{r}), \quad (8)$$

by

$$\Delta n_\lambda(\mathbf{r}) = \sum_{E_i < E_f} |\psi_i(\mathbf{r})|^2 - n_0 \quad (9)$$

or

$$\Delta n_\lambda(\mathbf{r}) = \frac{1}{\pi^2} \sum_{\ell=0}^{\infty} (2\ell+1) \int_0^{k_f} dk k^2 \left[|R_{\ell k}(\mathbf{r})|^2 - |J_\ell(kr)|^2 \right] + 2 \sum_b |\psi_b(\mathbf{r})|^2, \quad (10)$$

where $\psi_b(\mathbf{r})$ refers to the bound state wave functions and E_f and k_f are the Fermi energy and Fermi wave vector respectively. The effective potential, $V_{\text{eff}}(\mathbf{r})$ is given by

$$V_{\text{eff}}(\mathbf{r}) = -\phi(r) + \frac{\delta E_{\text{xc}}[n(\mathbf{r})]}{\delta n(\mathbf{r})}, \quad (11)$$

where $\phi(\mathbf{r})$ is the total electrostatic potential of the system and $E_{\text{xc}}[n(\mathbf{r})]$ is the exchange correlation energy of the system. For the exchange-correlation contribution to the effective potential in Eq. (11) we use the expression given by Hedin and Lundqvist [18], in atomic units (double Rydbergs):

$$V_{\text{xc}}(\mathbf{r}) \equiv \frac{\delta E_{\text{xc}} n(\mathbf{r})}{\delta n(\mathbf{r})} = -0.02908 \left[\frac{21}{r_s} + 0.7734 \ln \left(1 + \frac{21}{r_s} \right) \right],$$

where $(4/3)\pi r_s^3 = 1/n$.

In order to have $V_{\text{eff}}(\mathbf{r})$ vanishing at large \mathbf{r} , the exchange correlation part is rescaled to

$$V_{\text{xc}}(\mathbf{r}) \rightarrow V_{\text{xc}}[n(\mathbf{r})] \rightarrow V_{\text{xc}}[n(\mathbf{r})] - V_{\text{xc}}[n_0] \quad (12)$$

We carried out the calculation of $\Delta n_\lambda(\mathbf{r})$ following the method of Manninen *et al.* [19]. For more details the reader may see Refs. 15 and 19. Notice that the calculation has to be done for each value of λ between zero and one.

3. Phonon Dispersion Curves

We followed the work of Boccara and Sarma [20] with the extensions given by Gillis *et al.* [21] and Cowley and Shukla [22].

We present here the resulting set of self-consistent equations to solve within the self consistent harmonic approximation. For more details the reader may see Ref. 20, 21 and 22.

The set of equations to be solved is

$$w_\lambda^2(\mathbf{k})E_\lambda^\alpha(\mathbf{k}) = \sum_\beta D_{\alpha\beta}(\mathbf{k})E_\lambda^\beta(\mathbf{k}), \quad (13)$$

where $E_\lambda^\alpha(\mathbf{k})$ is the α component of the polarization vector $E_\lambda(\mathbf{k})$ and the dynamical matrix is

$$D_{\alpha\beta}(\mathbf{k}) = \frac{1}{M} \sum_\ell (1 - \cos(\mathbf{k} \cdot \mathbf{R}_\ell)) \langle \phi_{\alpha\beta}(\mathbf{R}_\ell) \rangle, \quad (14)$$

with

$$\begin{aligned} \langle \phi_{\alpha\beta}(\mathbf{R}_\ell) \rangle &= \frac{1}{(8\pi^3 \det \lambda_\ell)^{1/2}} \\ &\times \int d^3 u \exp \left(-\frac{1}{2} \sum_{\gamma\delta} u_\gamma (\lambda_\ell^{-1})_{\gamma\delta} u_\delta \right) \phi_{\alpha\beta}(\mathbf{R}_\ell + \mathbf{u}_\ell), \end{aligned} \quad (15)$$

where M is the ion mass, \mathbf{u}_ℓ is the vector describing the displacement of atom ℓ from its equilibrium position \mathbf{R}_ℓ and $\phi_{\alpha\beta}(\mathbf{R}_\ell + \mathbf{u}_\ell)$ is the tensor derivative of the interatomic potential evaluated at $\mathbf{R}_\ell + \mathbf{u}_\ell$. Finally,

$$\begin{aligned} (\lambda_\ell)_{\alpha\beta} &= \frac{1}{MN} \sum_{k\lambda} (1 - \cos(\mathbf{k} \cdot \mathbf{R}_\ell)) \\ &E_\lambda^{*\alpha}(\mathbf{k}) E_\lambda^\beta(\mathbf{k}) \coth \left[\frac{(1/2)\beta\hbar w_\lambda(\mathbf{k})}{\omega_\lambda(\mathbf{k})} \right], \end{aligned} \quad (16)$$

where N is the number of ions. The sum is over the first Brillouin zone, β is $1/k_B T$, with k_B being the Boltzmann constant.

To solve the set of self consistent Eqs. (13), (14), (15) and (16) and obtain the phonons we start with the frequencies generated by the Harmonic Approximation as the first guess. Then, the convergence procedure is followed.

4. Results and Discussion

As the first step we obtained the densities fully self consistently by numerically solving the Schrödinger equation. To solve this equation we used four blocks with different step size in each of them. In the first block we used a step size of $0.01a_0$, where a_0 is the Bohr radius ($a_0 = 0.529 \text{ \AA}$) up to $R = 1.7a_0$. The second block goes from $R = 1.7a_0$ to $R = 5.1a_0$ with a step size of $0.02a_0$. The third block goes from $R = 5.1a_0$ to $R = 11.9a_0$ in steps of $0.04a_0$ and finally the fourth block goes from $R = 11.9a_0$ to $R = 25.5a_0$ in steps of $0.08a_0$. The phase shifts were evaluated at $R = 25.5a_0$. The sums over ℓ in Eq. (10) were ended at $\ell_{\max} = 9$. The values of the phase shifts are shown in table I. Notice how the last four phase shifts are practically zero. The corresponding Friedel Sum Rule is also shown in table I. The discrepancy between the obtained value and correct value of the Friedel Sum Rule was of only 0.016%. The convergence in the value of the effective potential and in the value of the electronic density was of one part in 10^6 between consecutive iterations. Figure 1 shows the resulting density for $\lambda = 1$. We made the numerical calculation for 13 different values of λ . The step size in λ was $1.0/13.0$

With the calculated densities for the set of values of λ , we calculated the interionic potential using Eq. (5). The resulting potential is shown in Fig. 2.

From the calculated potential we obtained the phonons using the self consistent harmonic approximation. The phonon dispersion curve we obtained is shown in Fig. 3. We can see that the predicted phonons are very far from the experimental ones, which are shown in Fig. 4. However, they have the same overall shape as experimental

$$r_s = 2.06406a_0;$$

$$a_0 = 0.529 \text{ \AA}$$

$$\text{FSR} = 13.002141$$

$$n_0 = 6.616076;$$

$$n_1 = 3.950931$$

$$n_2 = 0.322911;$$

$$n_3 = 0.037282$$

$$n_4 = 0.006463;$$

$$n_5 = 0.001296$$

$$n_6 = 0.000290;$$

$$n_7 = 0.000083$$

$$n_8 = 0.000055;$$

$$n_9 = 0.000050$$

TABLE I. Values of the phase shifts, n_l , for aluminum. The values of r_s (metal density parameter) and of the Friedel Sum Rule (FSR) are also given.

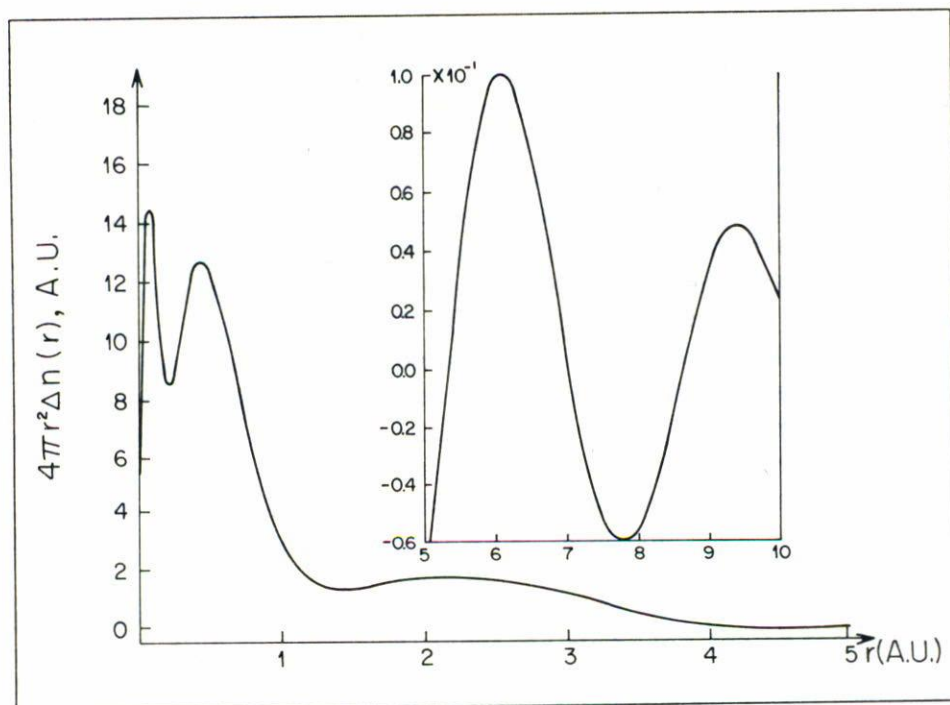


FIGURE 1. Electronic density around an aluminum ion in aluminum metal.

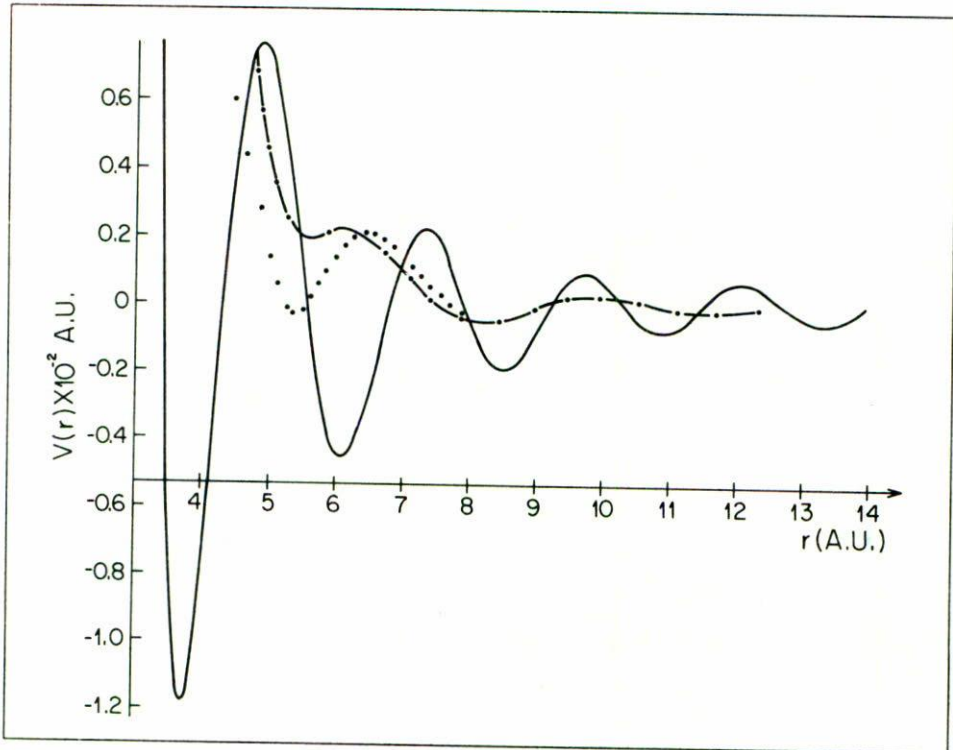


FIGURE 2. Interionic potential in aluminum. From this work: — ; from Ref. 9: .. ; from Ref. 7: — . — .

results. The maximum frequency predicted is about a factor of seven larger than the corresponding experimental one.

The calculation of the phonon dispersion curve included 22 neighbouring shells. The frequencies were converged to within one percent. The temperature was taken with the values of 0°K , 10°K , and 300°K without any significant changes in the result.

In the case of lithium for which this same approach was taken in order to calculate the interionic potential and the phonon dispersion curve [15], the difference between the predicted phonons and the corresponding experimental results is about 40%. It is clear that for aluminum which is a heavier metal the predictions get worse. So, for

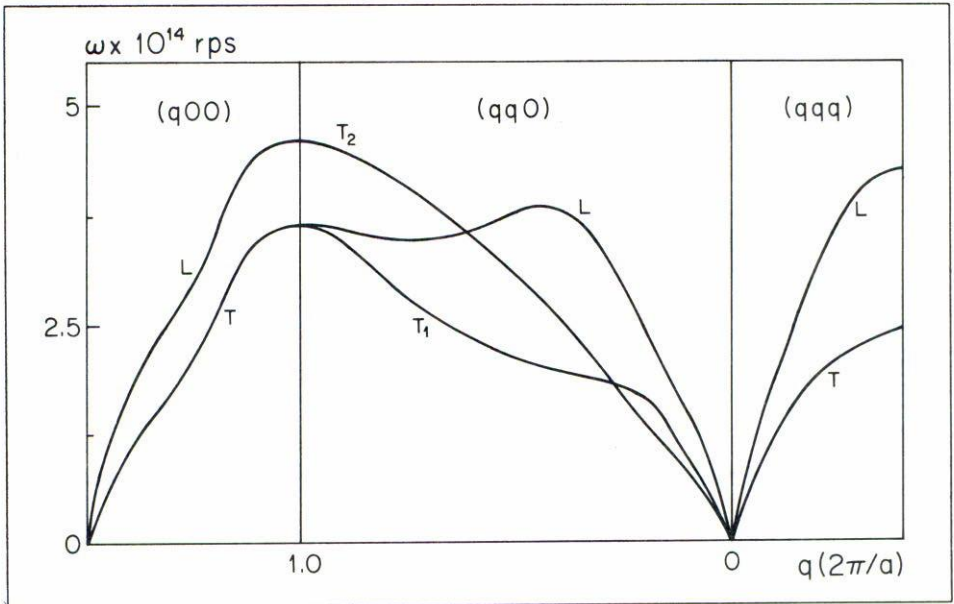


FIGURE 3. Calculated phonon dispersion curve for aluminum.

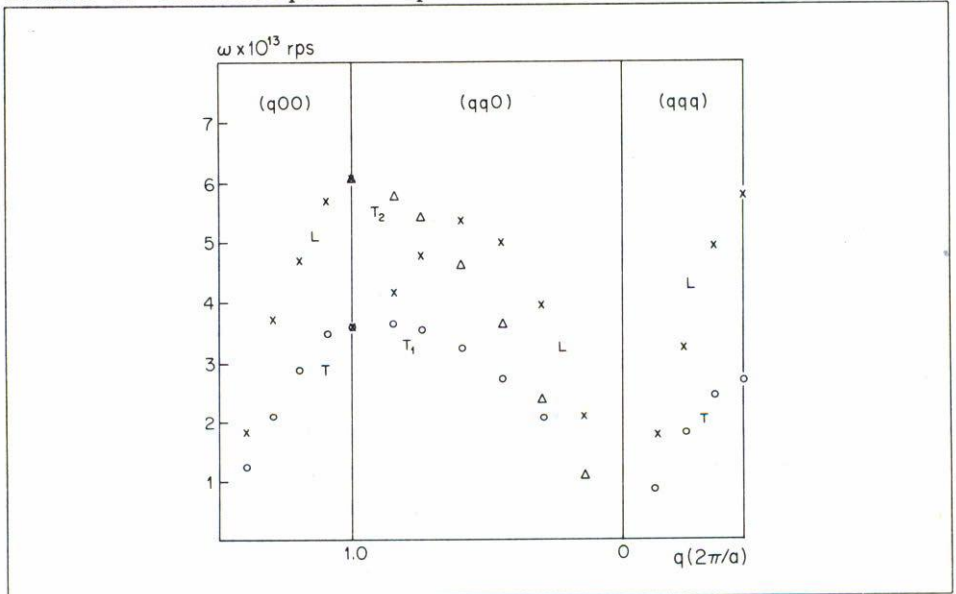


FIGURE 4. Experimental phonon dispersion curve for aluminum.

aluminum this approach to find the interionic potential is no longer useful. However, the validity of this method had to be explored for metals heavier than hydrogen and lithium.

Superposing the two displaced charge densities, at the origin and at \mathbf{R} (see Eq. (4)) is a major approximation (which is common to the usual perturbation theory approach) and is the part that we feel has to be improved to take a more realistic interionic charge density. There are exchange-correlation effects between the two clouds of electrons around each ion which were not taken into account when using Eq. (4). These effects become more important for metals with heavier nuclei. Finding the electronic charge densities for two centres of force would be the best way of getting a more realistic interionic charge density and this is a difficult problem to solve. But if this problem could be solved the method, which does not have any adjustable parameter and is a very pure ab initio calculation, should give a potential very close to the real one.

References

1. L.F. Magaña, M.D. Whitmore, J.P. Carbotte, *Can. J. Phys.* **60** (1982) 424.
2. R.A. Johnson, *J. Phys. F* **3** (1973) 295.
3. H.O. Pomuk and T. Halicioglu, *Phys. Status Solidi A* **37** (1976) 694.
4. J.K. Lee, J.A. Barker, F.F. Abraham, *J. Chem. Phys.* **58** (1973) 3166.
5. M.I. Blaskes and C.F. Melius, *Phys. Rev. B* **20** (1979) 3197.
6. A.E. Carlsson, M.L. Klein, H. Erenreich, *Philos. Mag. A* **41** (1980) 241.
7. M. Rasolt, R. Taylor, *Phys. Rev. B* **11** (1975) 2717.
8. L. Dagens, M. Rasolt, R. Taylor, *Phys. Rev. B* **11** (1975) 2726.
9. M. Manninen, P. Jena, R.M. Nieminen, J.K. Lee, *Phys. Rev. B* **24** (1981) 7057.
10. W.A. Harrison, J.M. Wills, *Phys. Rev. B* **25** (1982) 5007.
11. A.K. Gupta, P. Jena, K.S. Singwi, *Phys. Rev. B* **18** (1978) 2712.
12. H. Hohenberg, W. Kohn, *Phys. Rev.* **136** (1964) B964.
13. W. Kohn, L.J. Sham, *Phys. Rev.* **140A** (1965) 1133.
14. L.F. Magaña, *Phys. Lett.* **80A** (1980) 193.

15. G.J. Vázquez, L.F. Magaña, *J. Phys.* **46** (1985) 2197.
16. R.C. Shukla, *J. Chem. Phys.* **45** (1966) 4178.
17. R.P. Feynman, *Phys. Rev.* **56** (1939) 340.
18. L. Hedin, B.I. Lundqvist. *J. Phys. C* **4** (1971) 2064.
19. M. Manninen, R. Nieminen, P. Hautojarvi, J. Arponnen, *Phys. Rev. B* **12** (1975) 4012.
20. W. Boccara and G. Sarma, *Physics* **1** (1965) 219.
21. N.S. Gillis, N.R. Werthamer, T.R. Koehler, *Phys. Rev.* **165** (1968) 951.
22. E.R. Cowley, R.C. Shukla, *Phys. Rev. B* **9** (1974) 1261.